

Figure 13. Probability distribution function $\Delta v(n)$ for different pure water simulations: (a) $\nu(n)_{3w} - \nu(n)_{3w}$; (b) $\nu(n)_{1w^*} - \nu(n)_{3w}$.

Figure 13 and a comparison between Figures 7 and 12 indicate that a 10% decrease in the density may explain half the difference in the water-water interaction between simulations 1b and 2b. Thus, the effect from different water density, if any, is not sufficient to explain the differences in Figures 7 and 8 between the cluster model and simulations with periodical boundary conditions.

The cluster model suffers from the truncation of all interactions at the sphere boundary. However, this can be at least partly compensated for by solvating the cluster in a dielectric continuum. The difference in solvation energy for the water cluster and the water + benzene cluster may be divided into two parts: one arising from the difference in cluster radii and a second one due to the presence of the benzene molecule. The solvation energy for a pure water cluster with a radius R is given by

$$U^S(R) = \gamma \cdot A \quad (6)$$

and for a cluster with radius R and ΔR

$$U^S(R + \Delta R) = \gamma' A' = (\gamma + \Delta\gamma)(A + \Delta A) \approx \gamma A + \gamma \Delta A + \Delta\gamma A \quad (7)$$

where we have omitted the term quadratic in Δ . The term A in eq 6 and 7 is the area of the cluster and γ the surface internal energy, which for H_2O is somewhat larger (0.118 J/m^2) than the surface free energy (0.072 J/m^2) at room temperature.³⁷ Thus, the second term on the rhs of eq 7 will give a 19.1 kJ/mol more exothermic solvation energy when changing the radius from 10.86 to 10.96 Å. It is, however, considerably more difficult to estimate the change in the surface tension due to the change in radius.³⁸⁻⁴⁰

(37) Davies, J. T.; Rideal, E. K. "Interfacial Phenomena"; Academic Press: New York and London, 1963.

Following the ideas of Benson and Shuttleworth,⁴⁰ one may estimate this contribution to be $< 1 \text{ kJ/mol}$. The other part, which may be viewed as the difference in relaxation energy between the cluster model and an infinite system, can be estimated in a continuum approximation, and it is found to be negligible ($\leq 1 \text{ kJ/mol}$). Thus, we find that neither a change in the water density nor simple continuum corrections in the cluster model are able to explain the discrepancy between the different solvation energies found in this model and the model with periodic boundary conditions.

The dependence on the structure in pure water of boundary conditions has earlier been investigated by Pangali et al.²⁷ In a comparison between a cubic and a spherical cutoff with periodic boundary conditions, they found that the number of hydrogen bonds was larger in the latter case. They also found that the structure was heavily dependent on the cutoff distance. Thus, from their and our studies, it seems crucial to use the same boundary conditions when making comparative investigations, although still effects from the boundary conditions may not be negligible.

Conclusions

The benzene-water pair potential shows a rather strong orientation dependence mainly due to the dipole-quadrupole interaction. This preferential orientation is also reflected in the orientation of water molecules in the first hydration shell of benzene. The water structure is only slightly perturbed by the presence of the benzene molecule, although both a first and a second hydration shell are discernable.

However, the main observation from our simulations is that different boundary conditions may lead to quite different results. This is certainly true for global properties like the solvation energy and maybe to a lesser extent for more local properties like the benzene-water distribution functions, confined to the first hydration shell. Neither of the two models considered is able to reproduce experimental results for the solvation energy, and there does not seem to be any obvious choice of model. Further methodological studies are certainly warranted.

Acknowledgment. P.L. acknowledges a grant from Stiftelsen Bengt Lundquists Minne.

Registry No. Water, 7732-18-5; benzene, 71-43-2.

(38) Tolman, R. C. *J. Chem. Phys.* **1949**, *17*, 333.

(39) Kirkwood, J. G.; Buff, F. P. *J. Chem. Phys.* **1949**, *17*, 338.

(40) Benson, G. C.; Shuttleworth, R. *J. Chem. Phys.* **1951**, *19*, 130.

Aqueous Hydration of Benzene

G. Ravishanker, P. K. Mehrotra, M. Mezei, and D. L. Beveridge*

Contribution from the Hunter College of the City University of New York, New York, New York 10021. Received October 12, 1983

Abstract: A (T, V, N) ensemble Monte Carlo computer simulation has been performed on a dilute aqueous solution of benzene at 25 °C. The calculation employs intermolecular pairwise potential functions determined from quantum mechanical calculations. The results are analyzed by means of the proximity criterion, which permits the hydration to be described on a solute atom or molecular fragment basis. The results indicate the first solvation shell hydration complex of benzene consists of some 23 water molecules. The in-plane hydration is found to be essentially hydrophobic. The π -cloud hydration involves a first shell of two water molecules situated one above and one below the molecular plane, and the nature of interaction has both hydrophilic and steric attributes. Results are discussed in comparison with recent simulation studies of alkyl groups.

In view of the importance of the hydrophobic effect in structural biochemistry, a knowledge of the details of the hydrophobic hydration of prototype apolar species at the molecular level is quite

desirable. Recent research studies from this laboratory have employed liquid-state computer simulations to study the structure and energetics of dilute aqueous solutions of CH_4 ,¹ a prototype

for hydrophobic hydration, and the potential of mean force between CH_4 molecules in aqueous solution,^{2,3} a prototype system for hydrophobic interaction. From the results of these studies, the essential clathrate-like nature of the hydrophobic hydration complex, expected from the early Frank–Evans “iceberg” ideas,⁴ was further delineated. Relatively high first shell coordination numbers were found to be a common characteristic of hydrophobic hydration and were identified with water cage effects. Such contributions were also recognizable in the aqueous hydration of CH_3 , CH_2 , and CH groups in polyfunctional solutes studied by computer simulation.⁵ To the extent these results are transferable, one can infer the structure of hydration complexes for amino acid residues in alanine, valine, leucine, isoleucine, and, to some extent, proline.

Other amino acid residues such as phenylalanine and tryptophan as well as the nucleotide bases adenine, guanine, thymine, cytosine, and uracil involve unsaturated organic ring structure. These moieties are typically classified as hydrophobic, although the situation is possibly more complex than that for alkyl group hydration since the polarizability of the π -electron cloud admits the possibility of hydrophilic hydration above and below the molecular plane as well as in interactions involving the heteroatoms. An important prototype aqueous hydration problem for this class of molecules is the dilute aqueous solution of benzene, $[\text{C}_6\text{H}_6]_{\text{aq}}$. Benzene is of course only sparingly soluble in water. The thermodynamics of transfer have been determined and are $\Delta G = +5.33$ kcal/mol and $\Delta S = -15.7$ cal/(deg·mol) as quoted by Edsall and McKenzie.⁶ Evidence of specific benzene–water interactions comes from studies by Backx and Goldman,⁷ who observed nonclassical rotational behavior of D_2O in water/benzene solutions and anticipated a weak hydrogen bond between H_2O and the benzene π -electron cloud. Though there has been experimental work on the hydrophobic interaction of benzene molecules,⁸ there is little known at the molecular level about the nature of benzene hydration. To explore the aqueous hydration of the phenyl group and to determine the nature of the hydrophobic and hydrophilic effects in this system, we have extended our computer simulation studies to $[\text{C}_6\text{H}_6]_{\text{aq}}$ at 25 °C.

While this work was in progress, Karlström et al.⁹ reported a new theoretical determination of an intermolecular potential function for the benzene–water interactions using quantum mechanical calculations. A novel means of correcting for the basis set superposition error was introduced. Comparison of the Karlström et al. results with those of the potential function used for our study gives an indication of the sensitivity of calculated interaction energies to basic assumptions in the theoretical methodology.

Calculations

Statistical thermodynamic (T, V, N) ensemble Monte Carlo calculations were carried out on $[\text{C}_6\text{H}_6]_{\text{aq}}$ with use of a modified Metropolis procedure¹⁰ incorporating the force bias method¹¹ and

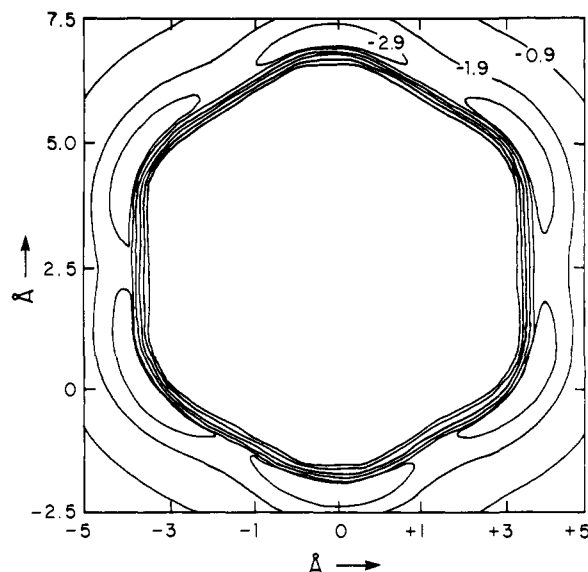


Figure 1. Isoenergy contour surface for benzene–water dimer in the molecular plane of benzene. Lowest energy is labeled A and corresponds to -2.9 kcal/mol. Each successive contour increases in energy by 1.0 kcal/mol.

preferential sampling¹² for convergence acceleration. The system for study was comprised of 216 rigid particles, one benzene molecule, and 215 water molecules. The simulation was performed at a temperature of 25 °C and a density determined from the experimentally observed partial molar volume of water and benzene.⁸ The condensed-phase environment of the system was provided by means of face centered cubic periodic boundary conditions, which provide in excess of two complete hydration shells for the solute. Convergence characteristics and statistical error bounds on each of the calculated quantities were monitored by control functions based on the method of batch means. Full details of the Monte Carlo methodology are given in a recent article by Mehrotra et al.¹⁰

The N -particle configurational energies of the system were calculated under the assumption of pairwise additivity in intermolecular interactions with use of potential functions determined from ab initio quantum mechanical calculations. For the water–water interactions we continue to use the MCY–CI(2) potential¹³ developed by Matsuoka et al. and representative of moderately large configuration interaction calculations on the water dimer. For the calculation of benzene–water interactions, a potential function was constructed from the 12–6–1 functional form, and the transferable parameters were determined from minimal basis set LCAO–SCF–MO calculations by Clementi et al.¹⁴ The net charges on C and H were taken to be -0.2 and 0.2 , respectively, obtained from molecular orbital calculations using Clementi’s basis set in the GAUSSIAN-80 system of programs.

The performance of the MCY–CI(2) water–water potential is now well documented.¹⁵ Simulations based on this potential are well-known to underestimate the internal energy of liquid water by 12%, about the amount expected by the neglect of cooperative effect in assuming pairwise additivity. A wide range of thermodynamic, structural, and dynamical properties of liquid water are well described in simulations based on this potential. Particularly excellent agreement is obtained with experiment on the

(1) Swaminathan, I.; Harrison, S. W.; Beveridge, D. L. *J. Am. Chem. Soc.* **1978**, *100*, 5705.

(2) Ravishanker, G.; Mezei, M.; Beveridge, D. L. *Symp. Faraday Soc.* **1983**, *17*.

(3) Beveridge, D. L.; Ravishanker, G.; Mezei, M. In “Structure and Dynamics of Proteins and Nucleic Acids”; Clementi, E., Sarma, R. H., Eds.; Adenine Press: New York, 1983.

(4) Frank, H. S.; Evans, M. J. *J. Chem. Phys.* **1945**, *13*, 507.

(5) (a) Marchese, F. T.; Mehrotra, P. K.; Beveridge, D. L. In “Biophysics of Water”; Franks, F.; Mathias, S., Eds.; Wiley: New York, 1982. (b) Marchese, F. T.; Mehrotra, P. K.; Beveridge, D. L., submitted for publication in *J. Phys. Chem.* (c) Mezei, M.; Mehrotra, P. K.; Beveridge, D. L., manuscript in preparation.

(6) Edsall, J. T.; McKenzie, H. A. *Adv. Biophys.* **1978**, *10*, 137.

(7) Backx, P.; Goldman, S. *J. Phys. Chem.* **1981**, *85*, 2975.

(8) (a) Dutta-Choudhury, M. K.; Mlljevic, N.; Van Hook, W. A. *J. Phys. Chem.* **1982**, *86*, 1711. (b) Tucker, E. E.; Christian, S. D. *Ibid.* **1979**, *83*, 426. (c) Tucker, E. E.; Lane, E. H.; Christian, S. D. *J. Solution Chem.* **1981**, *10*, 1.

(9) Karlström, G.; Linse, A.; Wallqvist, A.; Jonsson, B. *J. Am. Chem. Soc.* **1983**, *105*, 3777.

(10) Mehrotra, P. K.; Mezei, M.; Beveridge, D. L. *J. Chem. Phys.*, **1983**, *78*, 3156.

(11) Pangali, C.; Rao, M.; Berne, B. *J. Chem. Phys. Lett.* **1978**, *55*, 413.

(12) (a) Mol. Phys. **1979**, *37*, 1773. (c) *J. Chem. Phys.* **1979**, *71*, 129.

(13) (a) Owicki, J. C.; Scheraga, H. A. *Chem. Phys. Lett.* **1979**, *47*, 600.

(b) *J. Am. Chem. Soc.* **1977**, *99*, 7413.

(14) Matsuoka, O.; Clementi, E.; Yoshimine, M. *J. Chem. Phys.* **1976**, *64*, 1351.

(15) Clementi, E.; Cavallone, F.; Scordamaglia, R. *J. Am. Chem. Soc.* **1977**, *99*, 5531.

(16) Beveridge, D. L.; Mezei, M.; Mehrotra, P. K.; Marchese, F. T.; Ravishanker, G.; Vasu, T. R.; Swaminathan, S. In “Molecular-Based Study and Prediction of Fluid Properties”; Haile, J. M., Mansoori, G., Eds.; American Chemical Society: Washington, DC, 1984; Adv. Chem. Ser.

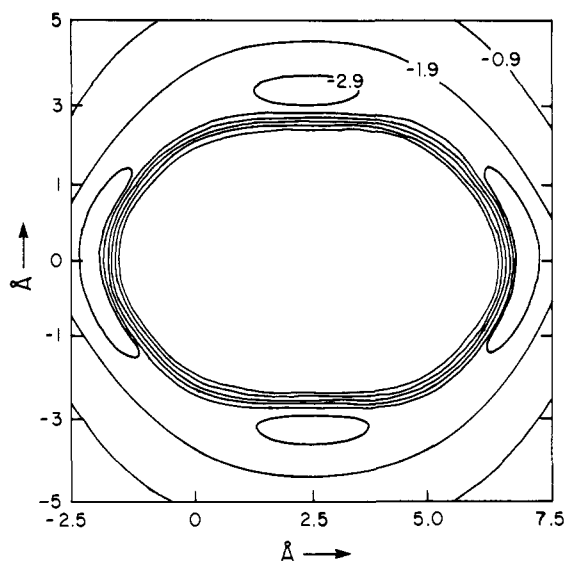


Figure 2. Isoenergy contour surface for benzene-water dimer in the plane perpendicular to the molecular plane of benzene. Lowest energy is labeled A and corresponds to -2.9 kcal/mol. Each successive contour increases in energy by 1.0 kcal/mol.

oxygen-oxygen radial distribution function, indicating essential structural elements of the system are well accommodated. The principal problem with the potential is the curvature in the region of equilibrium water-water separations, which leads to an inordinately high calculated pressure. The general position of Monte Carlo simulations on the liquid water problem is described in a recent review article by Beveridge et al.¹⁵

For the benzene-water potential, no direct test of quality is available. Slices of the potential energy hypersurface for the benzene-water interaction computed from the potential used in this study are shown Figures 1 and 2. Benzene-water interaction energies in the molecular plane (Figure 1) and perpendicular to the molecular plane (Figure 2) are found to be worth ~ 3 kcal/mol of stabilization energy. The function recently developed by Karlström et al.⁹ shows a similar placement of in-plane and out-of-plane energy minima in the benzene-water surface, with corresponding energy minima of -1.9 and -2.9 kcal/mol, respectively. The discrepancy in the out-of-plane interaction energy as computed by the two approaches is quite small. The difference in the in-plane binding energy, ~ 1 kcal/mol, is not expected to influence the results on solution structure from the simulation, but the effect of such a difference on energetics is more complicated to predict and will be discussed below. The benzene-water interaction energies in both cases are slightly greater than the 1 kcal/mol found for methane-water interactions and less than the 5 kcal/mol intermolecular hydrogen bond between water molecules. The benzene-water stabilization energy is therefore in a range reasonable for a hydrophobic-like dipole-induced dipole interaction or a weakly hydrophilic hydrogen bonding interaction.

In the computer simulation, all potential functions for water-water interactions were truncated at a spherical cutoff of 7.75 Å, whereas the benzene-water interaction energies were treated under the minimum image convention. No solute-solute interactions are included, and the simulated system then corresponds to a dilute aqueous solution.

The complete simulation involved a total of $1700K$ configurations. The initial configuration was a random distribution of non-overlapping particles. The initial $700K$ configurations of the sampling were treated as equilibration and were discarded, and ensemble averages were formed over the remaining $1000K$ configurations. The convergence profile for the calculation is shown in Figure 3.

Results

The calculated internal energies and related quantities for $[C_6H_6]_{aq}$ are collected in Table I. The quantities entered here are the mean energy U of the system ($N_S = 1$, $N_W = 215$), the

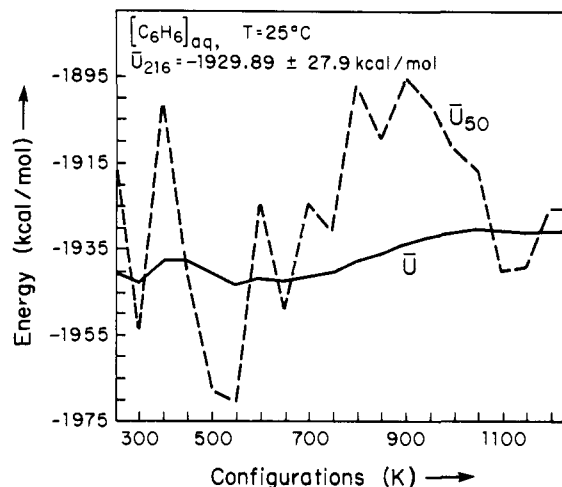


Figure 3. Convergence profile for the force-bias, preferential sampling augmented Monte Carlo simulation on $[C_6H_6]_{aq}$. Mean energy is denoted as \bar{U} , and mean energy for batches of size $50K$ is denoted as \bar{U}_{50} .

Table I. Calculated Internal Energies for the Dilute Aqueous Solution of Benzene at $25^\circ C$ in kcal/mol^a

	A ^b	B ^c
U_{SW} ($N_W = 215$; $N_S = 1$)	-1929.89	-1861.59
U_W ($N_W = 215$)	-1859.75	-1859.75
U_W' ($N_W = 215$)	-1869.29	-1864.42
\bar{U}_S'	-60.60	2.83
\bar{U}_{rel}	-9.55	-4.77
\bar{U}_S	-70.15	-1.86

^a See ref 1 for definition of these terms. ^b Results from simulation as described in Calculations. ^c Results from simulation based on benzene-water potential with the attractive region set everywhere to 0.

energy U_W of 215 water molecules in $[H_2O]_1$ at $25^\circ C$, U_W' , the corresponding energy of solvent water in $[C_6H_6]_{aq}$, \bar{U}_S , the calculated partial molar internal energy of transfer for C_6H_6 into water, and finally \bar{U}_S' and \bar{U}_{rel} , the solute-solvent and solvent-solvent contributions to U . Each of these is formally defined in eq 1-12 and Figure 4 of a previous paper from this laboratory by Swaminathan et al.¹ The calculated molecular distribution functions and analysis thereof for $[C_6H_6]_{aq}$ at $25^\circ C$ follow. The analysis formalism follows that described by Mehrotra and Beveridge,¹⁶ except where noted. The results are displayed first on a solute atom-by-atom basis, then developed in terms of C-H and C_6 fragments, and finally extended to indices referred to the entire C_6H_6 solute molecule. The interpretation and implications of the results are discussed in the following section.

The solute atom-solvent water radial distribution functions are described in the following paragraphs. Two forms of these functions are presented for each atom: (a) a "total" solute atom-water radial distribution function, $g_{AW}^{tot}(r)$, conventionally defined, and (b) a solute atom-water $g_{AW}^{1^0}(r)$, describing only those solvent water molecules designated "primary" to the solute atom based on the proximity criterion, i.e., those waters closer to that atom than to any other. This $g(r)$ is renormalized to the volume element of the truncated spherical shell of the Voronoi polyhedron associated with the primary region of the solute atom.¹⁷ The $g_{AW}^{tot}(r)$ and $g_{AW}^{1^0}(r)$ are collected for each solute atom on a single graph, together with the corresponding running coordination numbers.

The calculated solute-water radial distribution functions of the benzene carbon and hydrogen atom in $[C_6H_6]_{aq}$ are shown in Figure 4. All solute atom-water radial distribution functions refer to the center of mass of water molecules unless otherwise noted. The total $g_{CW}(r)$ and the $g_{CW}^{1^0}(r)$ for carbon, symmetry averaged over the six carbon atoms, and the corresponding running

(16) Mehrotra, P. K.; Beveridge, D. L. *J. Am. Chem. Soc.* **1980**, *102*, 4287.

(17) Mezei, M.; Mehrotra, P. K.; Beveridge, D. L. *J. Biomol. Struct. Dynamics*, in press.

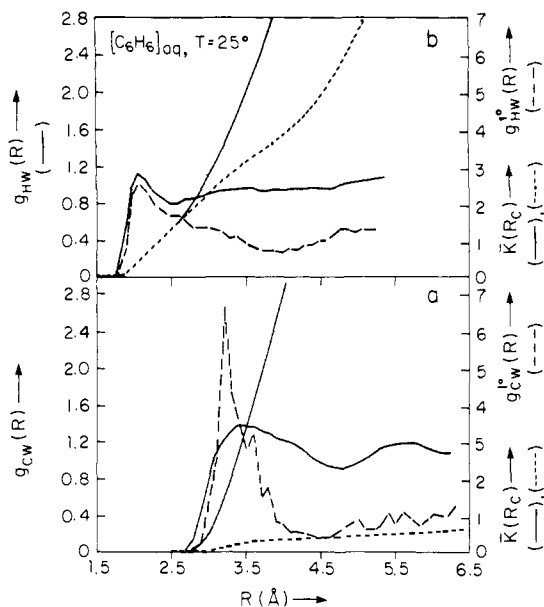


Figure 4. Calculated total (—) and primary (---) solute-solvent radial distribution functions and the corresponding running coordination numbers on an atom-by-atom basis in $[\text{C}_6\text{H}_6]_{\text{aq}}$. These distributions are symmetry averaged over six carbon atoms (a) and six hydrogen atoms (b) of benzene.

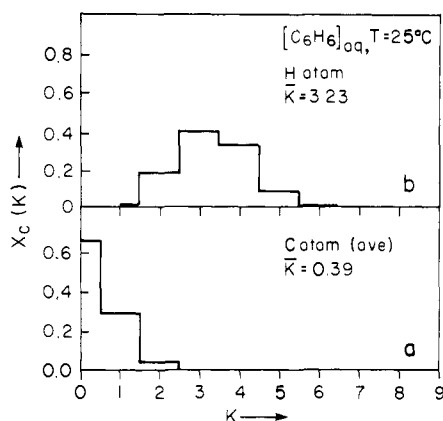


Figure 5. Calculated symmetry-averaged QCDF for primary solute-solvent coordination number on an atom-by-atom basis in $[\text{C}_6\text{H}_6]_{\text{aq}}$.

coordination numbers are given in Figure 4a. The total $g_{\text{CW}}(r)$ shows two peaks, each relatively broad, since both in-plane and out-of-plane solvent molecules are included together. The $g_{\text{CW}}^{\text{p}}(r)$ for carbon, by virtue of the proximity criterion, describes mainly those water molecules above and below the C_6 hexagon in benzene. A well-defined first shell with a maximum value at 3.2 Å is evident. Integrating this shell up to $r = 4.5$ Å gives a value of 0.37 water molecules per carbon atom in this region.

The total and primary radial distribution functions and running coordination number for the benzene hydrogen atom, also symmetry averaged, are shown in Figure 4b. The $g_{\text{HW}}^{\text{p}}(r)$ is of most interest and shows a maximum at 2.2 Å. The peak decays slowly to a minimum at 4.0 Å. The area under the curve indicates 3.42 waters are included in the first shell for each hydrogen. Here a composite of in-plane and out-of-plane solvation is reflected even in the $g_{\text{HW}}^{\text{p}}(r)$.

We turn now to an atom-by-atom analysis of the primary solvation of the carbon and hydrogen atoms of benzene in aqueous solution by means of quasicomponent distribution functions. This analysis is based on the $g_{\text{AW}}^{\text{p}}(r)$ and the R_{C} values discussed above. The distribution $x_{\text{C}}(K)$ of primary solvent coordination numbers K for benzene carbon and hydrogen atoms is shown in Figure 5. For the carbon atom, Figure 5a, the distribution ranges from zero to two with an average $\bar{K} = 0.39$. For hydrogen, Figure 5b, the distribution ranges from two to five, with three and four

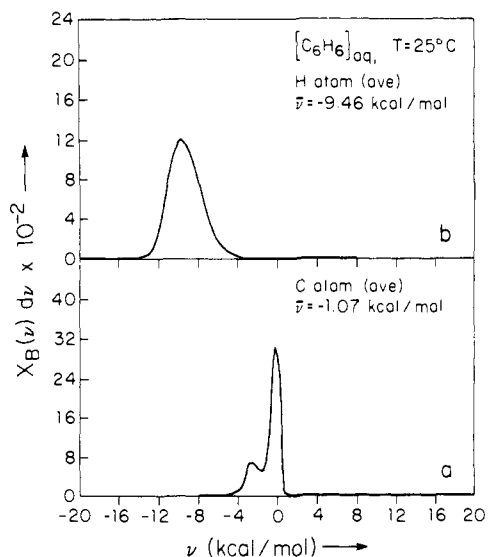


Figure 6. Calculated symmetry-averaged QCDF for primary solute-solvent binding energy on an atom-by-atom basis in $[\text{C}_6\text{H}_6]_{\text{aq}}$.

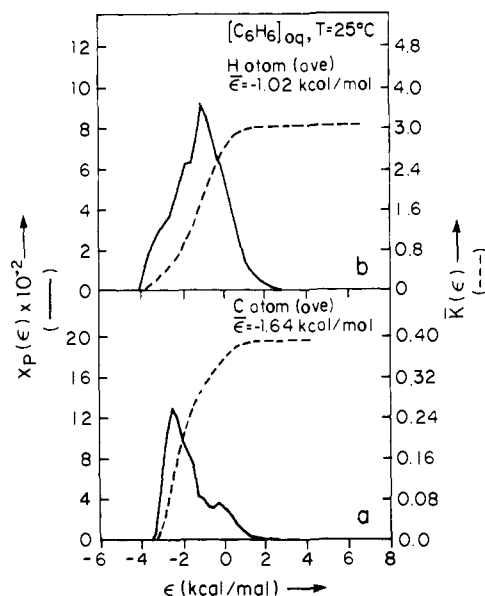


Figure 7. Calculated symmetry-averaged QCDF for primary solute-solvent pair energy on an atom-by-atom basis in $[\text{C}_6\text{H}_6]_{\text{aq}}$.

being the maximum contributors, and $\bar{K} = 3.23$.

The distribution $x_{\text{B}}(\nu)$ of binding energies for water molecules primary to the benzene atoms in $[\text{C}_6\text{H}_6]_{\text{aq}}$ is shown in Figure 6. For the carbon atom, Figure 6a, the distribution ranges from -4.5 to 0.5 kcal/mol with $\bar{\nu} = 1.07$ kcal/mol. For hydrogen the range is from -14.0 to -4.0 kcal/mol with $\bar{\nu} = -9.46$ kcal/mol.

The computed distribution functions $x_{\text{P}}(\epsilon)$ for solute-water pair interaction energy are given in Figure 7. For carbon, Figure 7a, the distribution ranges from -3.6 to 1.8 kcal/mol with the most probable ϵ value being -2.5 kcal/mol and with $\bar{\epsilon} = 1.64$ kcal/mol. For hydrogen, $x_{\text{P}}(\epsilon)$ ranges from -4 to 2.5 kcal/mol, with most probable ϵ value being -1.2 kcal/mol and $\bar{\epsilon} = -1.02$ kcal/mol. The out-of-plane benzene-water interactions are slightly stronger energetically than the in-plane interactions.

The above results can be combined to produce a description of the local solution environment of benzene in $[\text{C}_6\text{H}_6]_{\text{aq}}$ in terms of the C-H group and the C_6 fragment and also the entire C_6H_6 molecule. The groupwise distributions for coordination numbers, binding energies, and pair interaction energies are shown in Figures 8, 9, and 10, respectively. Of particular interest is the C_6 coordination number distribution, with contributions from $K = 0, 1, 2,$ and 3 and $\bar{K} = 2.34$. This shows that essentially one water

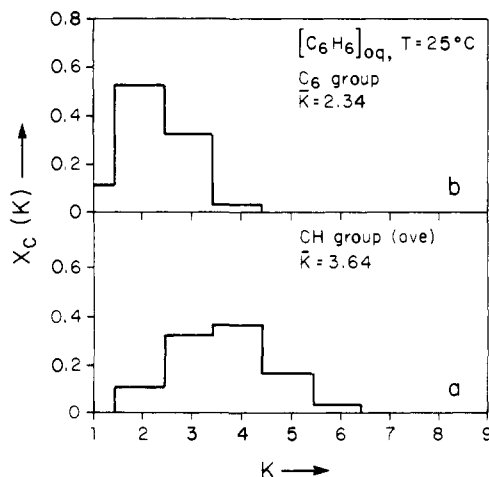


Figure 8. Calculated symmetry-averaged QCDF for primary solute-solvent coordination number on a functional group basis in $[\text{C}_6\text{H}_6]_{\text{aq}}$.

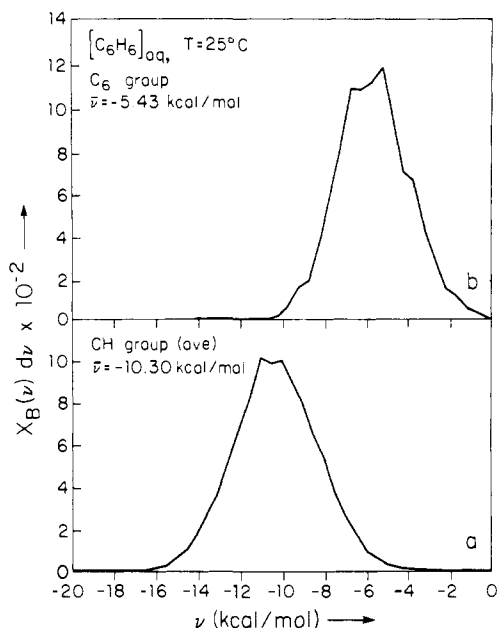


Figure 9. Calculated symmetry-averaged QCDF for primary solute-solvent binding energy on a functional group basis in $[\text{C}_6\text{H}_6]_{\text{aq}}$.

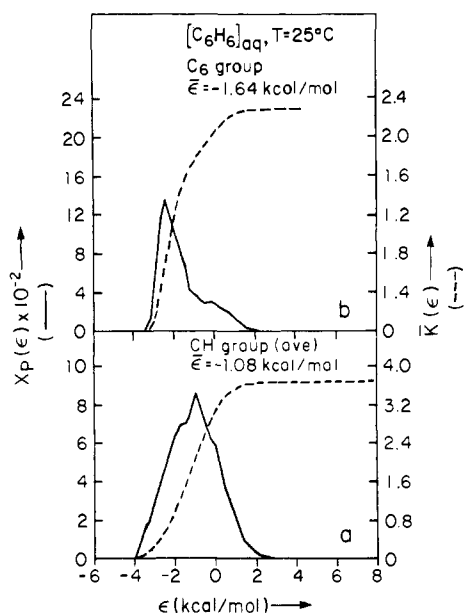


Figure 10. Calculated symmetry-averaged QCDF for primary solute-solvent pair energy on a functional group basis in $[\text{C}_6\text{H}_6]_{\text{aq}}$.

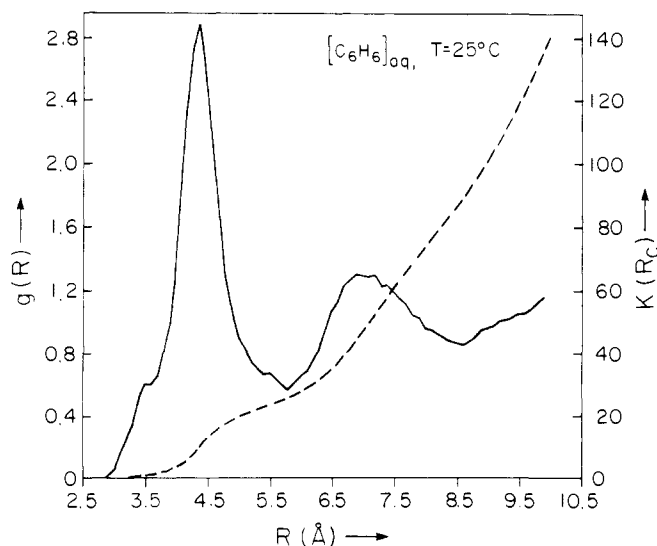


Figure 11. Calculated radial distribution function and the corresponding running coordination number on a molecular basis in $[\text{C}_6\text{H}_6]_{\text{aq}}$.

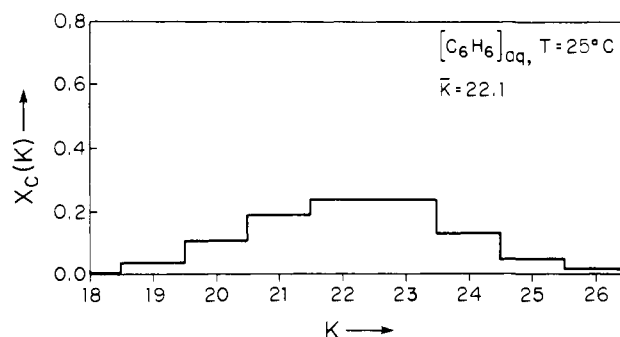


Figure 12. Calculated QCDF for primary solute-solvent coordination number on a molecular basis in $[\text{C}_6\text{H}_6]_{\text{aq}}$.

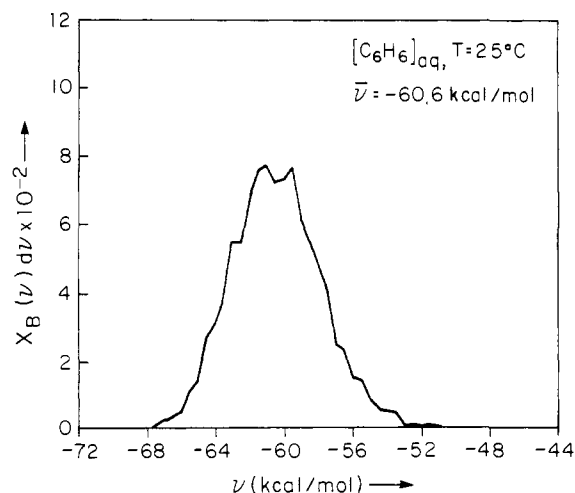


Figure 13. Calculated QCDF for primary solute-solvent binding energy on a molecular basis in $[\text{C}_6\text{H}_6]_{\text{aq}}$.

molecule above the plane and one below comprise the first hydration shell of the π cloud of benzene in $[\text{C}_6\text{H}_6]_{\text{aq}}$, with a corresponding pair interaction energy placed on the average at -3 kcal/mol and a distribution favoring bound values.

The distribution of the various analysis quantities referred to the entire molecule is shown in Figures 11–14. The first hydration shell of benzene is seen to involve from 19 up to 26 water molecules, with $\bar{K} = 22.1$. The average total binding energy for water molecules is -60.6 kcal/mol. The pair interaction energy extends from -3 to 0 kcal/mol, with the contribution at $\epsilon = 0$ coming from all the distant waters. The average pair energy is -1.08 kcal/mol.

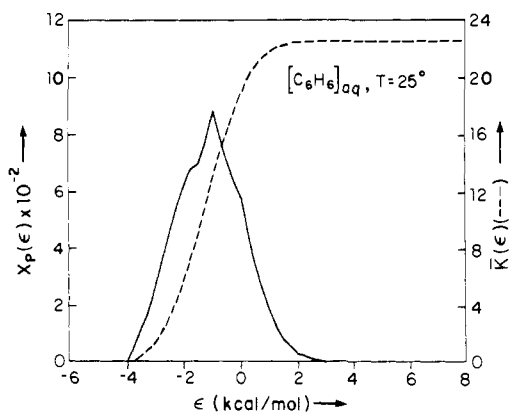


Figure 14. Calculated QCDF for solute-solvent pair energy and the running coordination number on a molecular basis in $[C_6H_6]_{aq}$.

Discussion

The essential structural feature of the aqueous hydration of benzene emerging from the simulation results is a first hydration shell consisting of 23 water molecules, shown in Figure 15. Twenty one of the first shell waters can be associated primarily with H-region hydration, and 2 are associated with hydration of the benzene ring above and below the carbon skeleton. Further insight into the nature of the calculated hydration can be obtained by examining details of the local hydration of the benzene ring C-H groups and π -electron cloud in individual structures contributing to the simulation. A stereoview of the computer-generated Dreiding model of the benzene hydration complex is shown in Figure 16; the "bonds" in the figure connect oxygen atoms of

water molecules that are within hydrogen bonding distance. This figure reveals the cage-like features of the benzene hydration complex. Quite a few puckered pentagonal forms can be discerned but so can contributions from higher and lower order polygonal forms. The irregularity of the polygons is a natural consequence of thermal disorder in the system at ambient temperatures. For the in-plane interactions, the number of waters and the spatial extent of the hydration shell are consistent with previous examples of hydrophobic hydration found in simulations on dilute aqueous solutions of alkyl group containing molecules. The average pair interaction energy of water molecules primary to the CH groups at -1.08 kcal/mol turns out to be significantly closer to corresponding values computed for methane-water interactions in $[CH_4]_{aq}$, suggesting that the apolar solute-water interactions are quite similar in both cases and essentially hydrophobic.

The hydration complex above and below the molecular plane, Figure 17, features two water molecules, one on each side of the benzene ring, located one above and one below the center of the π -electron cloud. A hydrogen atom on each water molecule extends into the π -cloud, toward the center of the molecule, and a mean pair energy of -1.64 kcal/mol is associated with this structure. The single water molecules interact with a set of second shell waters which extend over the carbon atoms and articulate with the H-region waters completing the benzene hydration. It is interesting to note that the in-plane and out-of-plane potential minima in the pairwise interaction energy surface, both 3 kcal/mol, give rise to quite different hydration structures in the simulation. The π -cloud hydration structure is favored by both a weak hydrogen bonding interaction and by steric factors, since the hydrogen atom of water can be accommodated better than the oxygen in the π cloud. The relative importance of these two effects is discussed below.

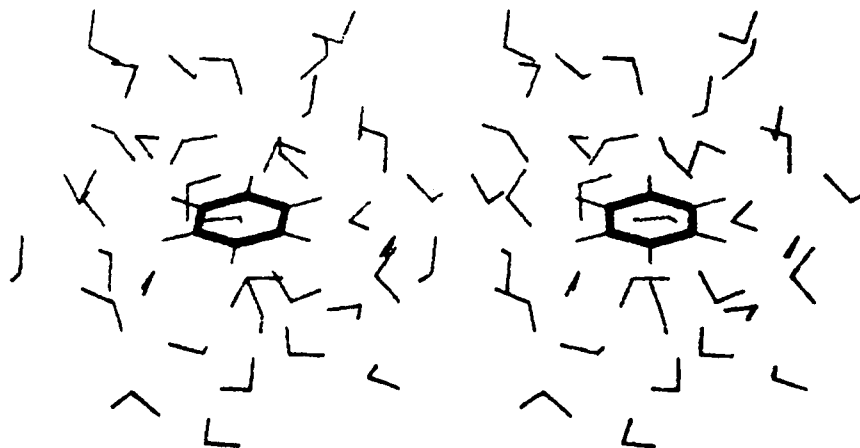


Figure 15. Stereographic view of a significant molecular structure contributing to the statistical state of $[C_6H_6]_{aq}$.

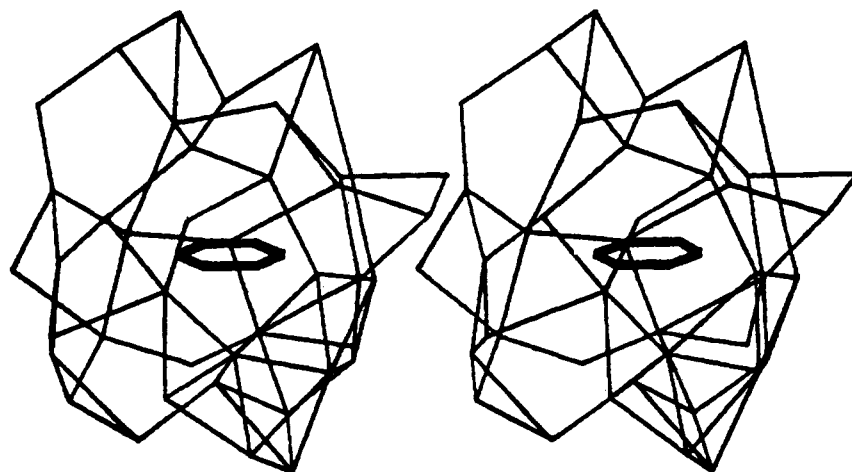


Figure 16. Stereographic view of the Dreiding model of the first hydration shell of benzene taken from the Monte Carlo simulation described herein on $[C_6H_6]_{aq}$ at 25 °C. Water oxygens within 3.2 Å are bonded.

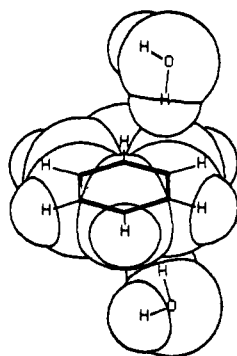


Figure 17. Space-filling model of benzene and two water molecules primarily belonging to the π cloud.

Partial molar internal energy of transfer for benzene calculated from simulation results comes out to be -70.15 kcal/mol with error bounds estimated to be ± 30.0 kcal/mol. This calculation used a value of -8.65 kcal/mol for the energy of water as calculated in a previous study.¹⁸ A recent, 3000K long run using the force-biased sampling scheme predicted a value of -8.75 kcal/mol for the energy of water.¹⁰ By use of this value, the partial molar internal energy of transfer of benzene is calculated to be -48.6 kcal/mol, with the estimated error bound still about ± 30.0 kcal/mol. The calculated transfer energy also has a large error associated with it because it is a small quantity derived from the difference of two large numbers known only with a considerable

(18) Mezei, M.; Swaminathan, S.; Beveridge, D. L. *J. Chem. Phys.* 1979, 71, 3366.

degree of statistical uncertainty. This number can also be expected to be quite sensitive to the well depth of the benzene-water interaction energy in the in-plane region. The energy difference of 1 kcal/mol between the function used herein and that of Karlstrom et al. propagated over 20 in-plane interactions could change the calculated transfer energy by 30%. Experience with similar problems in liquid water system¹⁵ indicates that the calculated structural characteristics of the system are not highly sensitive to small changes in energetics, and thus the description of the essential nature of the benzene hydration complex set forth herein is expected to remain valid.

Finally, we pursued the question of sensitivity of results to choice of potential function, with an additional simulation, identical with that previously described, except that the attractive part of the benzene-water potential was everywhere set to 0. The complete simulation also involved 1700K configurations with ensemble averages formed over the last 1000K. The computed energetics are given in column B of Table I. Here the transfer energy is reduced to -1.86 kcal/mol, still with large error bounds. Thus, the attractive part of the benzene-water potential influences the transfer energy significantly, with the experimental value bracketed by the two simulation results reported herein. The structural indices turned out to be essentially insensitive to this change in benzene-water potential, which indicates the steric contribution to the structure of the π cloud to be quite significant. Although a water hydrogen is proximal to the π cloud in this model, the nature of the interactions is not exclusively hydrophilic.

Further studies are underway to improve the quality of energetics in the potential function and in the simulation results, and determination of a potential of mean force for the benzene-benzene interaction is in progress.

Registry No. Benzene, 71-43-2; water, 7732-18-5.

Reactive Scattering of O(³P) with Toluene

R. J. Baseman,[†] R. J. Buss,[†] P. Casavecchia,[§] and Y. T. Lee*

Contribution from the Materials and Molecular Research Division, Lawrence Berkeley Laboratory, and the Department of Chemistry, University of California, Berkeley, California 94720. Received December 23, 1983

Abstract: In a crossed molecular beam study, the reaction of O(³P) + toluene, at 9.7 kcal/mol collision energy, is shown to give primarily radical products, CH₃ + phenoxy and H + cresoxy, under single-collision conditions. There is no evidence of intersystem crossing to a stable singlet species, cresol, as was previously observed in the O + benzene reaction. The isotropic angular distributions of the product suggest that the mechanism involves formation of a long-lived triplet biradical intermediate.

The chemical reactions of oxygen atoms with aromatic hydrocarbons remain only poorly understood in spite of efforts directed at elucidating the reaction mechanisms by many workers in the field. Knowledge of the mechanism of the initial reactions of these systems is important for understanding many combustion processes, but the bulk reactions are sufficiently complex, with highly reactive primary radical products producing secondary products, that identification of the primary mechanism is difficult in multicollision environments. For the prototypical reaction, O + benzene, the primary reaction channels were identified in a previous crossed molecular beam study¹ in which two competing reactions were observed. One channel, with products H atom and

phenoxy radical, is a simple substitution reaction which is similar to a major reaction occurring in many O(³P) + unsaturated hydrocarbon reactions. The second channel, which becomes more important at higher collision energies, is the production of a long-lived adduct, that is, the O-benzene triplet adduct appears to undergo collisionless intersystem crossing and rearrangement to singlet phenol which is sufficiently stable to live more than a millisecond in the absence of collisions and reaches the detector as an adduct. These results raise the question of when intersystem crossing will compete effectively with decomposition of the triplet adduct. The reaction of oxygen atoms with acetylene appears to involve similar processes.² If H atom migration on the triplet

[†] Fannie and John Hertz Foundation Graduate Fellow. Present Address: Sperry Univac, Semiconductor Division, St. Paul, MN 55164-0525.

* Present Address: Dept. 1811, Sandia National Laboratory, Albuquerque, NM 87185.

[§] Present Address: Department of Chemistry, University of Perugia, Perugia, Italy.

(1) Sibener, S. J.; Buss, R. J.; Casavecchia, P.; Hirooka, T.; Lee, Y. T. *J. Chem. Phys.* 1980, 72, 4341.

(2) Buss, R. J.; Baseman, R. J.; Casavecchia, P.; Hirooka, T.; Lee, Y. T. 8th International Symposium on Molecular Beams, Cannes, France, 1981. Baseman, R. J.; Buss, R. J.; Lee, Y. T. in preparation.